Automatic Change Detection in Very High Resolution Images with Pulse-Coupled Neural Networks

Fabio Pacifici, *Student Member, IEEE,* and Fabio Del Frate, *Member, IEEE*

***Abstract*—A novel approach based on Pulse-Coupled Neural Networks (PCNN) for image change detection is presented. PCNN are based on the implementation of the mechanisms underlying the visual cortex of small mammals and with respect to more traditional neural networks architectures such as Multi-Layer Perceptron (MLP) own interesting advantages. In particular, they are unsupervised and context sensitive. This latter property may be particularly useful when very high resolution images are considered, as in this case an object analysis might be more suitable than a pixel-based one. Qualitative and more quantitative results are reported. The performance of the algorithm has been evaluated on a pair of QuickBird images taken over the test area of Tor Vergata University, Rome.**

***Index Terms*— Pulse-coupled neural networks, unsupervised change detection, very high resolution images**

I. INTRODUCTION

World population growth affects the environment through the swelling of the population in urban areas and by increasing the total consumption of natural resources. Monitoring these changes timely and accurately might be crucial for the implementation of effective decision-making processes. In this context, the contribution of satellite and airborne sensors might be significant for updating land cover and land use maps. Indeed, the recent commercial availability of very high-resolution visible and near infrared satellite data has opened a wide range of new opportunities for the use of Earth observing satellite data. In particular, new systems such as the latest WorldView-1 [1], characterized by the highest spatial resolution, now provide additional data along with very high resolution (VHR) platforms, such as QuickBird or Ikonos, which have already been operating for a few years.

If on one side this permits the availability of a huge amount of information to yield always updated products, on the other side the need of completely automatic techniques able to manage big data archives is becoming extremely urgent.

According to what is already reported so far by previous studies, unsupervised change detection techniques mainly rely on three basic steps [2]. The first one is a pre-processing step where the images are spatially registered and some forms of radiometric standardization are also applied. In the second step a pixel-by-pixel comparison is usually performed, for example, using change vector analysis (CVA). In the third step one has to decide if the magnitude of the computed spectral changed vector exceeds some specified threshold criterion in order to conclude that some change has occurred.

However, most of the research carried out so far focused on medium or high spatial resolution images while only few studies have addressed the description of fully automatic change detection methods for VHR images. In these cases, several issues have to be specifically considered. The crucial ones include possible mis-registrations, shadow and other seasonal and meteorological effects which add up and combine to reduce the attainable accuracy in the change detection results. To emphasize the pixel contextual information, besides the spectral one, could be an appropriate approach to take these issues into account. Such an approach is indeed followed in [3], where the authors make progressive use of morphological filters based algorithms for the extraction of changed objects after CVA.

In this paper we consider a novel neural network approach for the detection of changes in multi-temporal VHR images. Neural networks (NNs) algorithms have been shown to be a rather competitive approach for image classification in remote sensing compared to other traditional approaches such as Bayesian or Support Vector Machines [4]. A supervised neural architecture based on MLPs has been recently applied to VHR images change detection with very highly accurate results [5] while a Hopfield-Type neural network technique for unsupervised change detection has been applied to Landsat Enhanced Thematic Mapper Plus (ETM+) imagery providing a positive performance [2].

Differently, the neural technique proposed in this paper is based on unsupervised pulse-coupled neural networks (PCNN) and is applied to VHR images. PCNN is a relatively new technique based on the implementation of the mechanisms underlying the visual cortex of small mammals [6]. The visual cortex is the part of the brain that receives information from

F. Pacifici and F. Del Frate are with Tor Vergata University, Computer Science, Systems and Production Engineering Department (DISP), Rome, 00133, Italy. (phone: +39-0672597734; e-mail: f.pacifici@disp.uniroma2.it, delfrate@disp.uniroma2.it).

the eye. The waves generated by each iteration of the algorithm create specific signatures of the scene which are successively compared for the generation of the change map. In terms of functionalities, this comparison is analogous to what is performed in the step 2 of the CVA. The advantage is that at this point step 3 is not necessary anymore, which significantly reduces the computational burden. Moreover, as it will be shown in next section, PCNN are characterized by using at the same time both contextual and spectral information which, as mentioned before, make them suitable for processing VHR images.

II. The PCNN Model

PCNN entered the field of image processing in the nineties, following upon the publication of a new neuron model introduced by Eckhorn *et al.* [6]. Interesting results have been already shown by several authors in the application of these models in image segmentation, classification and thinning [7, 8], including, in few cases, the use of satellite data [9, 10]. Hereafter we briefly recall the main concepts underlying the behavior of a PCNN while a more comprehensive introduction to image processing using PCNN is given in [11].

A PCNN is a neural network algorithm that, when applied to image processing, yields a series of binary pulsed signals, each associated to one pixel or to a cluster of pixels. It belongs to the class of unsupervised artificial neural networks in the sense that it does not need to be trained. The network consists of nodes with spiking behavior interacting each other within a pre-defined grid. The architecture of the net is rather simpler than most other neural network implementations. PCNN do not have multiple layers, which pass information to each other. PCNN only have one layer of neurons, which receive input directly from the original image, and form the resulting "pulse" image.

The PCNN neuron has three compartments. The feeding compartment receives both an external and a local stimulus, whereas the linking compartment only receives the local stimulus. The third compartment is represented by an active threshold value. When the internal activity becomes larger than the threshold the neuron fires and the threshold sharply increases. Afterwards, it begins to decay until once again the internal activity becomes larger. Such a process gives rise to the pulsing nature of the PCNN. The schematic representation of a PCNN is shown in Fig. 1 while, more formally, the system can be defined by the following expressions:

$$F_{ij}[n] = e^{-\alpha_F} F_{ij}[n-1] + S_{ij} + V_F \sum_{kl} M_{ijkl} Y_{kl}[n-1] \quad (1)$$

$$L_{ij}[n] = e^{-\alpha_L} L_{ij}[n-1] + V_L \sum_{kl} W_{ijkl} Y_{kl}[n-1] \quad (2)$$

where $S_{i,j}$ is the input to the neuron *(i,j)* belonging to a 2D grid of neurons, $F_{i,j}$ the value of its Feeding Compartment and $L_{i,j}$ is the corresponding value of the Linking Compartment. Each of these neurons communicates with neighbouring neurons *(kl)* through the weights given by *M* and *W* respectively. *M* and *W* traditionally follow very symmetric patterns and most of the weights are zero. *Y* indicates the output of a neuron from a previous iteration [*n*-1]. All compartments have a memory of the previous state, which decays in time by the exponent term. The constant V_F and V_L are normalising constants. The state of the feeding and linking compartments are combined to create the internal state of the neuron, *U*. The combination is controlled by the linking strength, β. The internal activity is given by:

$$U_{ij}[n] = F_{ij}[n]\{1 + \beta L_{ij}[n]\} \quad (3)$$

The internal state of the neuron is compared to a dynamic threshold, θ, to produce the output, *Y*, by

$$Y_{ij}[n] = \begin{cases} 1 \text{ if } U_{ij}[n] > \theta_{ij}[n] \\ 0 \quad \text{otherwise} \end{cases} \quad (4)$$

The threshold compartment is described as:

$$\theta_{ij}[n] = e^{-\alpha_\theta} \theta_{ij}[n-1] + V_\theta Y_{ij}[n] \quad (5)$$

when the neuron fires ($Y > \theta$), the threshold then significantly increases its value, this value decays until the neuron fires again. V_θ is a large constant that is generally more than one order of magnitude greater than the average value of *U*. Each neuron that has any stimulus will fire in the initial iteration, which, in turn, will create a large threshold value. It will then take several iterations before the threshold values decay enough to allow the neuron to fire again. The algorithm consists of iteratively computing (1) through (5) until the user decides to stop.

It is important to observe that the signal associated to the PCNN has properties of invariance to changes in rotation, scale, shift, or skew of an object within the scene [12]. This feature makes PCNN a powerful tool in change detection, where the view angle of the satellite can play an important role.

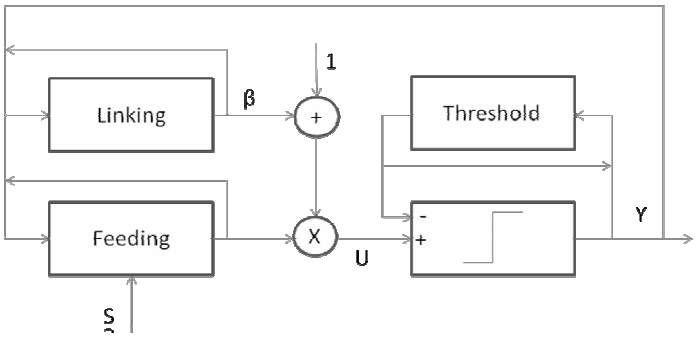

Fig. 1. Schematic representation of a PCNN

III. Application to Change Detection

The application of PCNN to change detection can be seen as a comparison of the PCNN outputs values corresponding to images acquired at different times. The response on the change occurrence stems directly from this comparison.

A first qualitative example is given by means of Fig. 2. Here we have three test areas, of different size, extracted from airborne very high resolution RGB images (about 20 cm) taken at two different times. In the first test area A we note very slight changes between the two acquisitions, basically consisting in some modifications occurred in the distributions of the plants in the garden. Note that we decided to consider a small area to assure high resemblance at the two different times. Test area B underwent, during the time shift, a few significant small scale changes even if the main structures are basically the same. Finally the test area C is extracted from test area B considering one of its most varied parts, shown by the red box in the test area B.

The idea is that PCNN can be used to individuate, in an unsupervised manner, the areas of an image where a significant change occurred. This can be obtained by measuring the similarity between the PCNN signal associated to the former image and the one associated to the latter. A rather simple and effective way to do this is to use a correlation function operating between the outputs of the PCNN. As we have an output value for each unit of the PCNN, i.e. for each pixel of the images, an average correlation value has to be computed in order to have a quick and global measure of similarity. This can be done by using the following expression:

$$G[n] = \frac{\sum_{ij} Y_{ij}[n]}{N}$$

where the sum includes all the pixels N of the image (or sub-image).

In Fig. 3 the PCNN output $G[n]$ for the considered test areas calculated as the mean over the three R, G, B bands is plotted while Table 1 reports the corresponding correlation values associated to each image pair. From Fig. 3 we see that the pulsing behavior of the two images of test area A is very similar. Both the waveform and the time dependence of the two signals appear to be highly correlated. For test area B the result changes. Here from the very first epochs the pulsing activity of the two images is rather different especially as far as the waveform is concerned. In test area C this difference still increases and also the time correlation seems to get lost very fast.

Such results are expressed more concisely by the correlation values reported in Table 1. It seems then that PCNN, once processing an image pair, might be capable to catch those portions where significant changes occurred. In such a context it seemed to us that an approach based on "hot spot" detection rather than on changed-pixel

TABLE I
NORMALIZED CORRELATION VALUES FOR THE THREE CONSIDERED TEST CASES

TEST AREA	CORRELATION VALUE
A	0.98
B	0.70
C	0.24

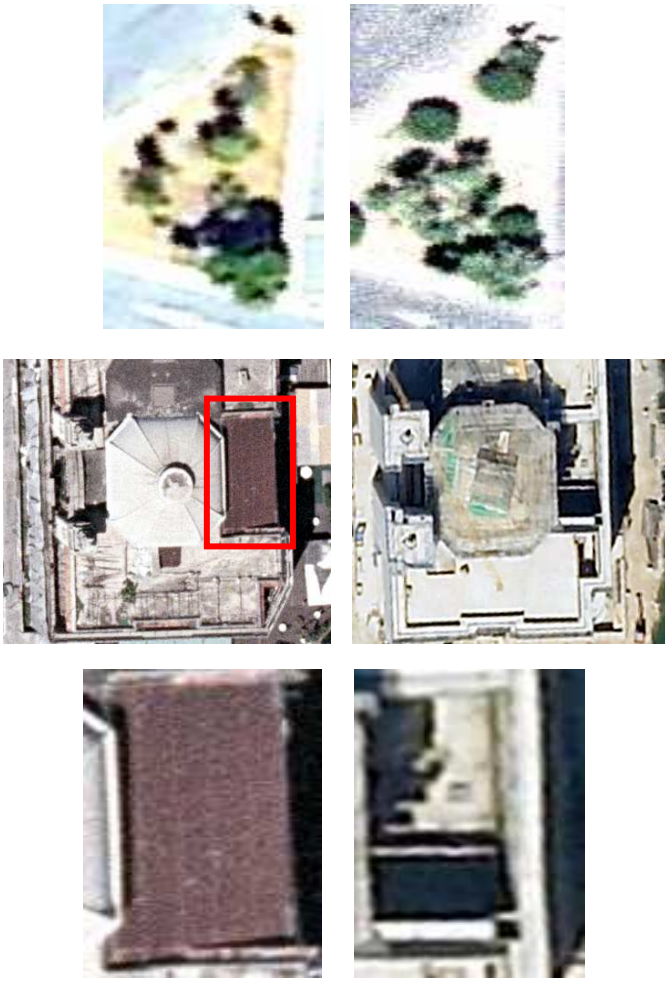

Fig. 2. Test areas A (up), B (middle), C (bottom) imaged at two different times t_1 (left) and t_2 (right)

detection could be more appropriate given the huge size of the images that we may need to analyse in next future. It is also true that, as it will be shown in next section, it is always possible to apply a multi-scale procedure to push the detection to finer spatial resolutions.

IV. Experimental Results

The accuracy of the presented technique has been evaluated more quantitatively applying it to a pair of QuickBird images taken on a selected test site. The area comprises the Tor Vergata University campus and its surroundings and is located in Rome, Italy. The two images have been acquired on 29-5-2002 and 13-3-2003 and

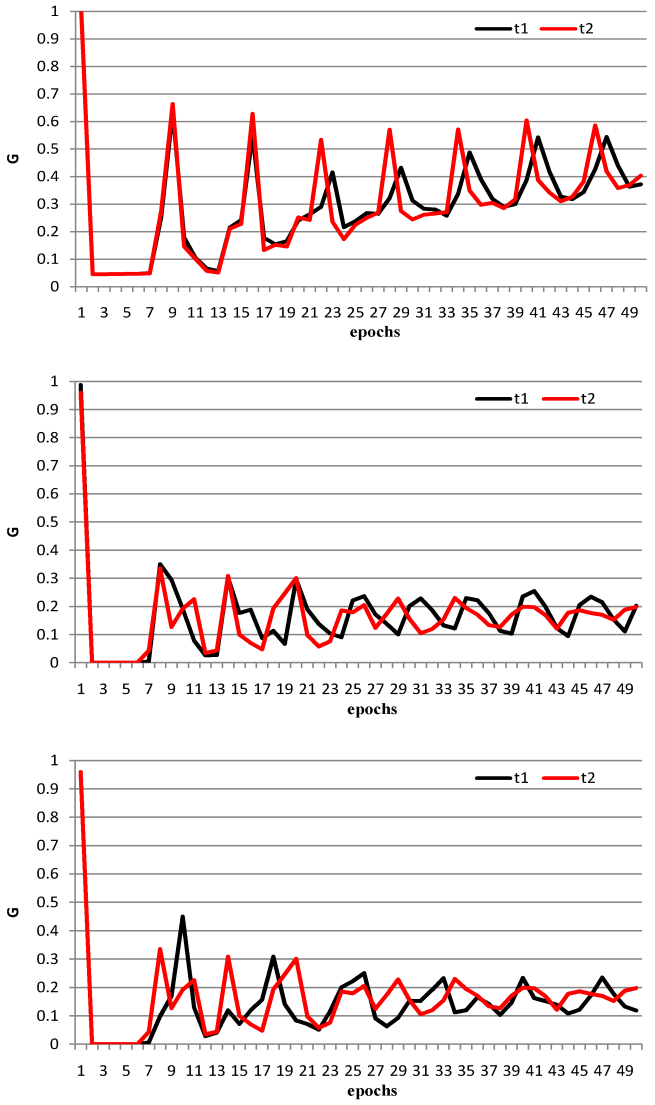

Fig. 3. PCNN signals of the images taken at two different times. Up: test area A, middle: test area B, bottom: test area C

underwent standard product pre-processing and co-registration. The panchromatic images have been considered in order to design a single PCNN working with higher resolution rather than 4 different ones processing lower resolution images. The two panchromatic images are shown in Fig. 4a and 4b. We can see that a few changes occurred in the area during the analysed time window, the main ones correspond to the construction of new commercial and residential areas. A complete ground-truth of the changes is reported in Fig. 4c. Note that the ground survey included also houses that were already partially built in 2002.

The size of the PCNN was of 100x100 neurons. For the reasons explained in the previous section we preferred working with lower resolution, only looking for the "hot spots" where a change could be rather probable. To operate in this way we averaged over the PCNN output values of the 10000 neurons belonging to 100x100 boxes. We actually considered an overlap between adjacent patches of 50 pixels (half patch). To increase the overlap would have meant to have more spatial resolution but at the price of an increase of the computational burden. Considering we are interested in detecting objects of at least some decades of pixels, we assumed that an overlapping size of 50 pixels could be a reasonable compromise. The computed mean correlation value was then used to discriminate between changed and not changed area.

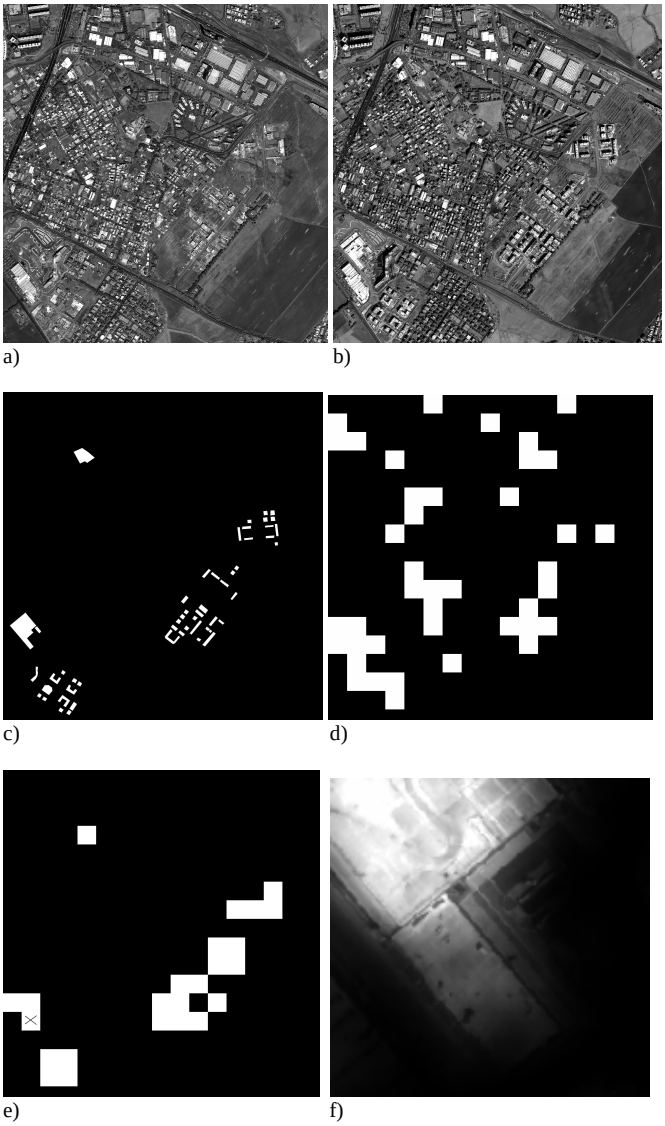

Fig. 4. a) panchromatic image (2825x2917 pixels) at time t_1. b) panchromatic image at time t_2.c) ground-truth. d) change detection result obtained by a standard image difference procedure. e) changed area as from the PCNN elaboration. f) pixel-based analysis carried out over one of the previously detected changed areas indicated with "x" in (e).

The result is shown in Fig. 4e while in Fig. 4d, for sake of comparison, we report the result obtained with a traditional image difference approach. More in detail, in this latter case, an average value has been computed for each box of the difference image and a threshold value to discriminate between changed and not changed areas selected. In Fig. 4d we have reported the result corresponding to a threshold value maximizing the number of true positives keeping reasonably low the number of false positives.

What should be firstly noted is that, at least in this application, the algorithm did not provide any intermediate outputs, with the correlation values alternatively very close to 0 or 1. This avoided to search for optimum thresholds to be applied for the final binary response. The accuracy is satisfactory, as 49 out of the 54 objects appearing on the ground-truth were detected with no false-alarms. The missed objects are basically structures that were already present in the 2002 image (e.g. foundations or the first few floors of a building), but not completed yet. On the other side one can see that the result given by a standard image difference technique, although a suitable threshold value was selected here, is rather imprecise, presenting a remarkable number of false alarms.

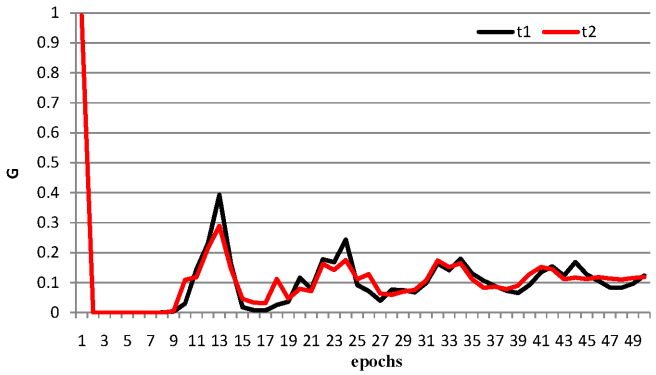

Fig. 5. PCNN signals corresponding to the patch indicated with "x" in Fig. 4e.

The image shown in Fig. 4f has been obtained by a multi-scale procedure. This consists in a new PCNN elaboration, this time on pixel basis, of one of the hot-spots generated with the first elaboration, in particular the one corresponding to the box indicated by the "x" in Fig. 4e. The pulsing activities of this box at the two considered different times are plotted in Fig. 5, in a way analogous to the plots of Fig. 3. A clear dissimilarity between the two waveforms, especially between epochs 9 and 25, can be observed. Finally it has to be noted that the output reported in Fig. 4f is more uniformly distributed within the range between 0 and 1. Its value has been multiplied with the panchromatic image taken at time t_2 to have a result which better exploits the VHR property of the original image.

V. Conclusion

The potential of a novel automatic change detection technique based on PCNN was investigated. PCNN belong to the family of NNs including a few interesting properties. They are unsupervised and context sensitive. Moreover they are invariant to an object scale, shift or rotation, which, once the two images are co-registered, might be rather useful especially for very high resolution images. The two waves, one for each image, generated by the PCNN during each iteration of the algorithm create specific signatures of the scene which can be compared for deciding about the occurrence of a change. Applying successively the procedure to a moving window allows the processing throughout the whole image.

We preferred an approach aiming at discovering changed subareas in the image rather than analyzing the single pixel. This might be more convenient when large data sets have to be examined, as it should be the case in the very next years when new satellite missions will be providing additional data along with the ones already available.

The application of the PCNN to a couple of QuickBird images taken over the Tor Vergata test site in Rome, Italy, with a time shift of less than one year, produced interesting results. An overall object accuracy of 90.7% has been obtained with no false-alarms. Moreover the method is rather fast as it directly analyses the correlation between the two signals associated to the images and no post-processing after the comparison is required to give the final response. Some investigations on the robustness of the settings of the PCNN parameters are currently ongoing. However, preliminary results indicate that applying the same parameters values considered for this paper to different VHR images keeps the performance still satisfactory. Regarding the single parameters, fluctuations around the chosen values seem to be more critical for V_θ and α_θ while β and α_L show a better stability.

References

[1] http://www.digitalglobe.com/index.php/86/WorldView-1

[2] S. Ghosh, L. Bruzzone, S. Patra, F. Bovolo, and A. Ghosh, "A context-sensitive technique for unsupervised change detection based on Hopfield-type neural networks," *IEEE Transactions on Geoscience and Remote Sensing*, vol. 45, no. 3, pp: 778-789, Mar. 2007

[3] M. Dalla Mura, J. A. Benediktsson, F. Bovolo, and L. Bruzzone, "An unsupervised technique based on morphological filters for change detection in very high resolution images," *IEEE Geoscience and Remote Sensing Letters*, vol. 5, no. 3, pp. 433-437, July 2008

[4] F. Pacifici, F. Del Frate, W. J. Emery, P. Gamba, J. Chanussot, "Urban mapping using coarse SAR and optical data: outcome of the 2007 GRS-S data fusion contest," *IEEE Geoscience and Remote Sensing Letters*, vol. 5, n. 3, pp. 331-335, July 2008

[5] F. Pacifici, F. Del Frate, C. Solimini, W.J. Emery, "An Innovative Neural-Net Method to Detect Temporal Changes in High-Resolution Optical Satellite Imagery", *IEEE Transactions on Geoscience and Remote Sensing*, vol. 45, n. 9, pp. 2940-2952, September 2007

[6] R. Eckorn, H. J. Reitboeck, M. Arndt, and P. Dicke, "Feature linking via synchronization among distributed assemblies: simulations of results from cat visual cortex," *Neural Computation*, vol. 2, pp. 293-307, 1990.

[7] G. Kuntimad and H. S. Ranganath, "Perfect image segmentation using pulse coupled neural networks," *IEEE Transactions on Neural Networks*, vol. 10, no. 3, May 1999.

[8] X. Gu, D. Yu, and L. Zhang, "Image thinning using pulse coupled neural network," *Pattern Recognition Letters*, vol. 25, pp. 1075-1084, 2004

[9] J. A. Karvonen, "Baltic sea ice SAR segmentation and classification using modified pulse-coupled neural networks," *IEEE Transactions on Geoscience and Remote Sensing*, vol. 42, no. 7, pp. 1566-1574, Jul. 2004

[10] K. Waldemark, T. Lindblad, V. Bečanović, J. L. L. Guillen, and P. Klingner, "Patterns from the sky satellite image analysis using pulse coupled neural networks for pre-processing, segmentation and edge detection," *Pattern Recognition Letters*, vol. 21, pp. 227-237, 2000

[11] T. Lindblad and J. M. Kinser, *"Image processing using pulse-coupled neural networks,"* Springer-Verlag, Berlin Heidelberg, 2005

[12] J. L. Johnson, "Pulse-coupled neural nets: translation, rotation, scale, distortion and intensity signal invariance for images," *Applied Optics*, vol. 33, no. 26, pp. 6239-6253, 1994